Int J Thermophys (2010) 31:556–571
DOI 10.1007/s10765-010-0740-x

Thermal Conductivity of Cobalt-Based Catalyst for Fischer–Tropsch Synthesis

Jianmin Wu · Haitao Zhang · Weiyong Ying · Dingye Fang

Received: 12 October 2009 / Accepted: 13 April 2010 / Published online: 7 May 2010

Abstract In this study, the thermal conductivity of cobalt-based catalyst specimens in the temperature range from 160 °C to 255 °C are measured via a steady-state apparatus. The apparatus and procedures are applied to several specimens of cobalt-based catalyst powder compacts. Specimens with different degrees of porosity are produced by pressing cobalt-based catalyst powder with a particle size of (80 to 360) mesh. The thermal conductivity of cobalt-based catalyst powder compacts is investigated as functions of temperature, specimen density, porosity, and powder size. The results indicate that the thermal conductivity of the catalyst specimens increases linearly with temperature and density and is practically independent of the particle size of the powder in an atmosphere of air, while the porosity dependence of the thermal conductivity is inverse to that of density. In addition, the effects of some measuring factors on the thermal conductivity show that the reliability of the thermal conductivity measurements of cobalt-based catalyst specimens are influenced easily by parallelism, specimen roughness, and moisture content, whereas the specimen thickness and water bath temperature have only a slight effect on the reliability.

Keywords Cobalt-based catalyst · Porosity · Steady-state method · Thermal conductivity

J. Wu (✉) · H. Zhang · W. Ying (✉) · D. Fang
State Key Laboratory of Chemical Engineering, Engineering Research Center of Large Scale Reactor Engineering and Technology, Ministry of Education, East China University of Science and Technology, Shanghai 200237, China
e-mail: wjmin@mail.ecust.edu.cn

W. Ying
e-mail: wying@ecust.edu.cn

List of Symbols

A_{Cu}	Cross-section area of copper heat probe (m^2)
A_S	Cross-section area of specimen (m^2)
L_1	Horizontal distance between two thermocouples welded on the lower heat probe (m)
L_2	Distance between the measuring end of the upper heat probe and thermocouples welded on the lower heat probe (m)
L_S	Thickness of specimen (m)
R	Correlation coefficient
R''	Total thermal resistance ($km^2 \cdot W^{-1}$)
t_1, t_2	Temperatures of the lower heat probe (°C)
t_3, t_4	Temperatures of the upper heat probe (°C)

Greek Symbols

λ	Thermal conductivity ($W \cdot m^{-1} \cdot {}^\circ C^{-1}$)
λ_{Cu}	Thermal conductivity of copper heat probe ($W \cdot m^{-1} \cdot {}^\circ C^{-1}$)
$\delta L_S / L_S$	Measuring error of specimen thickness
$\delta D / D$	Measuring error of specimen diameter
$\delta \Delta t / t$	Measuring error of temperature difference

1 Introduction

Heat transfer in heterogeneous fluid–solid systems is important in many types of processing—for example, catalytic reactors, heat exchangers, and thermal methods of oil recovery. A large amount of exothermic reaction systems of the gas–solid phase exist in petrochemical production; and the thermal conductivity of a catalyst is a critical parameter for describing the heat transfer properties of a system, especially for a highly exothermic reaction Ficher–Tropsch synthesis system. Accurate measurements of the thermal conductivity of a catalyst plays an important role in studying the variation regularity of internal catalyst concentration, temperature, and selectivity. Moreover, the thermal conductivity of a catalyst has a significant effect on reactor design, reaction process analysis, and optimization. Hence, determination of the thermal conductivity of a catalyst pellet as well as the relations between the thermal conductivity and particle size, particle density, and temperature by experimental measurements are of practical importance.

Since the physical meaning of the thermal conductivity was proposed by Fourier in 1822, a series of thermal-conductivity measurement methods for catalysts were advanced by many researchers [1–7]. Sehr [1] presented a comparison of three different measurement methods and the thermal conductivity of five different catalysts or carriers. Mischke and Smith [4] determined the effective thermal conductivity for several densities of alumina pellets under vacuum and atmospheric pressure using the spherical envelope method. Yu et al. [7] used a new steady-state method to measure the thermal conductivities of porous solid catalyst pellets. Measurements on other materials with different methods have been reported elsewhere [8–10].

Generally, there are two classical methods for measurements of the thermal conductivity on solids: (1) the steady-state methods in which the heat flow and temperature gradient are measured through a body of well-defined geometry, and (2) transient methods such as the transient hot-wire, the transient hot-strip, the transient plane-source, and the laser-flash method in which the time course of the temperature is measured when the boundary conditions on the object are suddenly changed. Both the steady-state and transient methods, however, may be used to measure the thermal conductivity of large, heterogeneous bodies consisting of catalyst dispersed in a suitable matrix. Although the usage of transient techniques has increased substantially in recent years, steady-state techniques such as the guarded hot-plate method, the steady-state heat flow method, the quasi-steady-state method, etc., are still widely used for the measurement of thermal conductivity. These methods, based directly on Fourier's law, require only measurements of base quantities such as length, diameter, temperature, electrical power, etc.

In this paper, the steady-state heat flow method, in which thermal equilibrium was attained in a few hours, was mainly introduced to measure the thermal conductivity of a cobalt-based catalyst specimen. The emphasis of the present work is on the experimental determination of the thermal conductivity of compacted specimens of cobalt-based catalyst powder as functions of density, powder particle size, porosity, and temperature in air under normal pressure. Moreover, the effects of some measuring factors on the reliability of thermal conductivity results are also considered to obtain the actual thermal conductivity of the cobalt-based catalyst. Determination of the above factor dependence of the thermal conductivity of a cobalt-based catalyst can be used to assess the roles of different factors in the heat transfer through a catalyst, and some other measuring factors are also considered. The use of the data to determine the temperature difference between the inside and outside of a catalyst during the process of a catalytic reaction is also of major significance.

2 Experimental

2.1 Thermal-Conductivity Apparatus

To carry out the investigations in the temperature range from 160 °C to 255 °C, a testing apparatus for measuring the thermal conductivity of specimens was designed and built for use in this work, and we carried out these measurements on cobalt-based catalysts. Hence, its design was based upon the so-called steady-state axial heat flow method. In this method, a fabricated specimen of unknown thermal conductivity is sandwiched between upper and lower heat probes, one of which is heated while the other is cooled to form the second constant temperature field. When steady-state conditions of operation are reached, it is assumed that the heat flow is one-dimensional and passes through the centerline of the specimen. With this assumption and measurements of the temperature, the unknown thermal conductivity is obtained.

A schematic diagram of the experimental apparatus is given in Fig. 1. The apparatus consists of a heating section, electrical control system, a cooling section, and

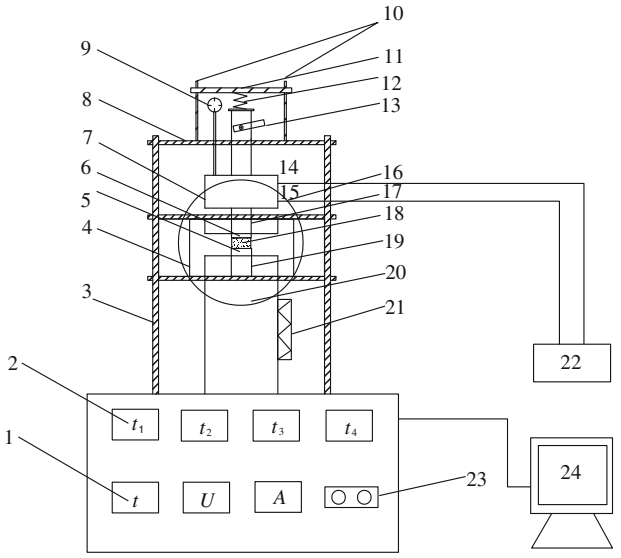

Fig. 1 Diagram of DRL-IIthermal conductivity apparatus: 1 Temperature controlling system, 2 Temperature display, 3 Stainless steel stand, 4 Cylindrical reflecting screen, 5, 6 Copper–constantan thermocouples, 7 Thermostatic water bath, 8 Top base, 9 Micrometer, 10 Bolts/nuts with an gasket, 11 Compression plate, 12 Springs, 13 Lifting handle, 14 Cooling water outlet, 15 Cooling water inlet, 16 Measuring region, 17 Upper heat probe, 18 Specimens, 19 Lower heat probe, 20 Main heater, 21 Protective heater, 22 Constant temperature water basin, 23 Switch system, 24 PC

computer system. The heating section includes a main heater, protective heater, the lower copper heat probe, thermocouples, and compression system.

The specified heat probe temperature was attained by means of an internal heater, which was surrounded by a stainless-steel cylinder to eliminate electrical connections through the specimen. From a knowledge of the heat input and the steady-state temperature distribution, the thermal conductivity could be computed. In operation, the heater controlled by a high precision and sensitive temperature-controlled meter produced an energy input for a stable heat probe temperature. Large diameter, insulated copper wire was used to attach the ends of the heater coil to the external power connections on the multipoint terminal board. A power source (220 V/50 Hz) was used, ensuring continuously adjustable and stable power inputs to these heaters. Meanwhile, a protective heater is set beside the main heater. The surface temperature difference of the two heaters is controlled to zero by a precision temperature control instrument in order to eliminate lateral temperature differences of the specimen. This design with a highly sensitive temperature measuring and control method ensures that all the energy produced from the main heater passes through the catalyst specimen axially. The energy was transferred to the specimen from the heat source through the copper heat probe axially, 30 mm in diameter, to reduce the radial heat losses and to ensure essentially uniform temperatures at the contact interfaces. The internal surface of each copper heat probe (in contact with the specimen) was sanded using very fine sandpaper and then polished, in order to minimize the surface roughness and, consequently, the thermal contact resistance. Two stainless-steel stands and three stainless-steel plates with

nominal diameters of 280 mm were specially designed to hold the combination of the specimen and the upper and lower heat probes together.

The measurement of the temperature was accomplished by means of four copper–constantan thermocouples, with 0.08 mm thickness thermal electrodes, which were welded to the surfaces of the upper and lower heat probes in parallel. The leads were cemented along the surface to reduce conduction errors. Such an arrangement greatly helped in precisely fixing the positions of the thermocouples. The horizontal distance between two thermocouples welded on the lower heat probe was 50 mm. And the distance between the measuring end of the upper heat probe and thermocouples welded on the lower heat probe was 1 mm. Meanwhile, the temperatures were displayed immediately on the temperature display ($t_1 - t_4$ in Fig. 1). The uncertainties in the temperature readings provided by the thermocouples were determined to be no more than 0.1 °C.

A stainless-steel cylinder, 12.5 cm in diameter and 2 mm in thickness, placed between two stainless steel base plates served as a reflecting screen around the upper and lower copper heat probes. This reflecting screen was used for minimizing the temperature difference and the radial heat losses, which encircled the path of heat flow. The axial heat losses of the heater were negligible.

The cooling section was constructed of a sealed cylindrical thermostatic water bath (12.5 cm in diameter, 9 cm in length, and 2.5 cm in thickness) of stainless steel through which water at a temperature of (40 ± 0.1) °C was circulated. Two orthogonal holes were bored on the surfaces of the body. These holes were fitted with 1.5 cm diameter plastic tubing, which served as coolant water inlet and outlet lines. Both lines extended through the same holes in the intelligent constant temperature water basin (THS-10), whose temperature was adjustable. It should be noted that the coolant flow lines were thoroughly sealed to the bath. An isothermal region was formed with the water circulation between the cooling constant temperature bath and the intelligent constant temperature water basin (THS-10) to provide a stable temperature at the cooling end.

The heating section, specimen, reflecting screen, and cooling section were held together (in compression mode) by means of three perforated circular stainless-steel plates and two stainless-steel stands. The compression plate ($10\text{mm} \times 50\text{mm} \times 160\text{mm}$) was kept horizontal using the regulating screw during the operation in order to read an accurate thickness of the specimen from the micrometer. The degree of compression of this assembly could be adjusted to desired values by changing the torque on the bolts/nuts combination. The flexibility provided by this overall design allowed the contact (compression) pressure at the interfaces between the specimen and heat probe to be increased externally: this compression was necessary in order to minimize the related thermal contact resistance. In addition, this compression system also helped to improve the thermal contact between the other sections of the apparatus. A high-thermal conductivity grease was also applied in a thin layer on both circular surfaces of the specimen and heat probes, in order to reduce the corresponding thermal contact resistances and ensure essentially one-dimensional heat conduction in the central region of the specimen. The experimental apparatus was also designed to meet some additional requirements: radiation and natural convection in the specimen had to be negligible compared to heat conduction; and all thermal contact resistance had to be minimized.

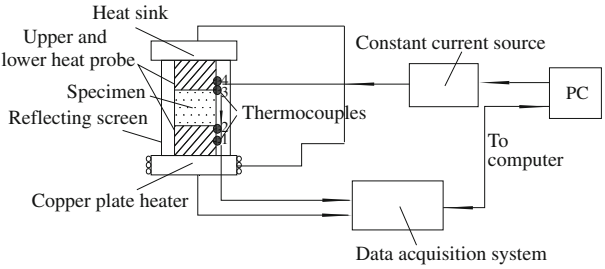

Fig. 2 Electrical block diagram of the measuring region

Because temperature measurements must be precise, it was important that the apparatus must be maintained in a carefully controlled environment. The external constant temperature water basin and thermostatic water bath were used to keep the apparatus temperature stable and minimize other effects resulting from temperature fluctuations.

Other equipments needed for operation of the apparatus are also shown in Fig. 1. The primary performance specifications of the thermal conductivity apparatus are as follows:

(1) Effective diameter: less than or equal to 30 mm
(2) Specimen thickness: 0.02 mm to 10 mm
(3) Temperature control range of lower heat probe: room temperature to 550 °C
(4) Temperature control range of upper heat probe: room temperature to 100 °C
(5) Measuring range of thermal conductivity: 0.01 $W \cdot m^{-1} \cdot °C^{-1}$ to 2 $W \cdot m^{-1} \cdot °C^{-1}$
(6) Power source: 220 V/50 Hz

Figure 2 shows a block diagram of the measuring region of the apparatus. The entire procedure was controlled by a personal computer (PC), which interacted with a constant current source and data acquisition system.

2.2 Specimen Preparation

Powdered cobalt-based catalyst particles were prepared by grinding egg-shell catalyst, whose mean diameter was 2.5 mm, and subsequent sieve analysis. The powders used were smaller than 80 mesh size and larger than 360 mesh size, which were uniaxially pressed at room temperature with a pressure from 10 MPa to 40 MPa, without binders.

Specimens of five different densities were prepared by compressing the powder in a hydraulic figuring machine (SDJ-5). Different masses of powder were poured into a cylindrical mold, 30 mm in inner diameter. In each case, the powder was compressed to give a disk specimen 30 mm in diameter and 2 mm to 10 mm thickness corresponding to a certain volume. From the known density of the cobalt-based catalyst and volume of the specimen, the volume fraction could be computed. Specimen disks, 2 mm to 10 mm in thickness and 30 mm in diameter, were used for specific heat measurements. Specimen preparation is a key link to assure the accuracy of the measurement results. The geometric dimension of commercial catalyst particles is relatively small. Therefore, in order to ensure a uniform temperature of the specimen and maintain good

Table 1 Specimens of different densities used to determine the thermal conductivity

Specimen number	Density ($g \cdot cm^{-3}$)	Theoretical density (%)	Estimated porosity (%)	Thickness (mm)	Diameter (mm)
1	0.9091	100.0	0	5.164	~30
2	0.8103	89.1	11.9	4.927	~30
3	0.7706	84.8	15.2	4.880	~30
4	0.7313	80.4	19.6	4.882	~30
5	0.6592	72.5	27.5	4.527	~30

contact with the heat probes, the specimen made of these catalyst particles must satisfy the following two requirements: (1) geometric dimension of catalyst specimen satisfies the measuring requirement of the apparatus, and (2) verticality between the bottom surfaces and the central axis of the specimen should be no more than 0.02 mm, and the roughness of the two ends of the specimen should be also less than 0.02 mm.

It was very difficult to achieve the requirements of the ends because of the random errors during the compression. So a thin coating of thermal grease was applied to both sides of the specimen and the upper and lower heat probes to minimize contact resistance between them. The properties of the specimens are given in Table 1.

Before the measurements were initiated, the specimen was first dried to a bone dry weight from 100 °C to 120 °C for more than 10 h to remove absorbed water.

2.3 Experimental Procedure

The measuring principle was based on Fourier's law. After the specimens were prepared, the following procedure was used in determining thermal-conductivity values.

First, before any specimens were measured in the cell, the micrometer reading for a zero specimen thickness was taken and the compression plate was removed from the apparatus by using the regulating screw. The thermal grease was applied in a thin layer between both sides of the heat probes and specimen. Next, the specimen was placed on the top of the lower heat probe as depicted in Fig. 1, and simultaneously the reflecting screen was pulled down in a sealed state. After the specimen was assembled along the specimen axes and the compression plate was screwed on by mechanical force, the micrometer reading was taken again and the zero reading subtracted to obtain the actual specimen thickness.

Each series of tests was initiated by turning on the power to the electrical heaters and starting the water circulation through the cooling section. The power input to the heaters and the flow rate and temperature of the cooling water ((40 ± 1) °C) were then set. The thermocouples were connected to a data acquisition and control system hooked to a PC. After this, data for the thickness and cross-section area of the specimen were input to a computer program and the heating switch was opened. Runs were then made at increasing temperature levels without permitting the specimen to cool between runs.

It should be noted that the present apparatus was more compact than a traditional steady-state apparatus such as the guarded hot-plate technique, and, therefore, it took less time to achieve a steady- state condition and to carry out the measurements. After the power supply to the heat probe was turned on, 2 h to 3 h were required for the heat flow to reach a steady state. A true steady state was never reached, as sinusoidal fluctuations in the bath temperature caused the temperature readings to vary about 0.1 °C. Temperatures were measured after a steady state was attained, and the thermal conductivity of the specimen was determined at a specific temperature. This was accomplished by reading the temperature on both faces of the specimen using the temperature display connected to the PC. Assuming negligible contribution of radiative and convective heat exchange, the following equation was used for calculation of the thermal conductivity according to Fourier's law

$$\lambda = \frac{A_{\mathrm{Cu}}}{A_{\mathrm{S}}} \frac{\lambda_{\mathrm{Cu}}(t_1 - t_2)L_{\mathrm{S}}}{L_1(t_2 - t_3) - L_2[(t_1 - t_2) + (t_3 - t_4)]} \tag{1}$$

where λ is the thermal conductivity of the specimen, λ_{Cu} is the thermal conductivity of the copper heat probe at a mean temperature, A_{Cu} is the cross-section area of the copper heat probe, A_{S} is the cross-section area of the specimen, t_1, t_2 are two different temperatures of the lower heat probe, t_3, t_4 are two different temperatures of the upper heat probe, L_{S} is the thickness of the specimen, L_1 is the horizontal distance between two thermocouples welded on the lower heat probe, and L_2 is the distance between the measuring end of the upper heat probe and thermocouples welded on the lower heat probe. Hence, the thermal conductivity of the specimen was calculated on the basis of the temperatures of the two ends of the specimen and the geometric dimensions of the specimen.

2.4 Error Analysis

The errors associated with thermal conductivity measurement methods have been discussed by several authors, and those for steady-state methods have been analyzed by Pillai and George [11], Longo [12], and Hammerschmidt [13]. Proceeding in a similar way, the relative errors of the apparatus were as given below.

L_{S}, D, t_1, t_2, t_3, and t_4 are independent variables. Considering the measurement errors to be random, the most probable error of the thermal conductivity according to Eq. 1 could be given by

$$\frac{\delta\lambda}{\lambda} = \sqrt{\left(\frac{\delta L_{\mathrm{S}}}{L_{\mathrm{S}}}\right)^2 + \left(\frac{\delta D}{D}\right)^2 + \left(\frac{\delta \Delta t}{t}\right)^2} \tag{2}$$

where $\delta L_{\mathrm{S}}/L_{\mathrm{S}}$ is the measuring error of the specimen thickness, $\delta D/D$ is the measuring error of the specimen diameter, and $\delta \Delta t/t$ is the measuring error of the temperature difference.

The errors of the micrometer and vernier caliper are 0.02 mm, and the precision of specimen thickness and diameter are 0.1 mm. Generally, the specimen thickness

is about 2 mm to 10 mm and the specimen diameter is about 30 mm. The uncertainty of the temperature difference between the two ends of the specimen is 0.1 °C, which mainly depends on the thermocouples and data acquisition system. The above values can be taken to be the error limit for the thickness, diameter, and temperature measurements. The errors derived from the apparatus themselves also have a slight effect on the measuring results. The main sources of experimental apparatus errors were radial heat exchange, thermal conduction along the thermocouples, and thermal expansion of the specimen. And hence, on the basis of Eqs. 1 and 2, the relative error of the apparatus was less than 5 %.

Probably the greatest error source in this investigation is the variation in temperature measurements. Therefore, the relative error of apparatus measurement was determined primarily by the accuracy with which the temperature gradients were measured, and these were functions of the thermal conductivity of the material. Some random errors of less significance resulted from measurements of the specimen thickness and diameter. The first type of error may be minimized by investigating a material of known thermal conductivity and then comparing experimental results with literature data.

3 Accuracy of Thermal-Conductivity Measurements

Since indeterminate errors cannot be quantified, the practical approach to assess the accuracy and reproducibility of any measuring equipment is to carry out measurements on standard materials and to identify the deviations from the reference values. Hence, the calibration of the apparatus was carried out on a specimen of Teflon, whose thermal conductivity was known in air. One of the specimens ($\rho = 1.95\,\mathrm{g \cdot cm^{-3}}$), a disk 29.6 mm in diameter and 8.38 mm in thickness, was investigated in the temperature range from 120 °C to 170 °C. The thermal conductivity of Teflon was plotted against temperature (Fig. 3).

A straight line was fitted to the data by means of a linear regression, and the value of Teflon thermal conductivity obtained at room temperature, 25 °C, was $0.216\,\mathrm{W \cdot m^{-1} \cdot {}^{\circ}C^{-1}}$. The dashed lines in Fig. 3 represent 95 % confidence limits about the regression

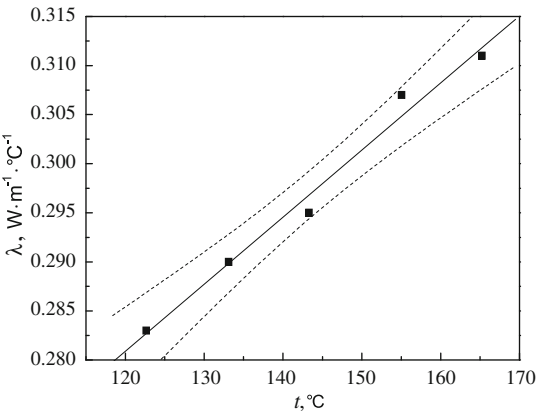

Fig. 3 Thermal conductivity of Teflon versus temperature

line. The relative error between literature [14] and experimental values was just about 4.6 %. This result showed excellent agreement with the standard value for Telfon.

The reproducibility of the data was verified with repeated measurements on the same specimen by successive measurements at different temperatures. It is possible to reproduce the thermal conductivity results within 5 % as determined by measurement on the most dense specimen. This specimen is subject to the largest errors because of the relatively high heating rate and small temperature gradient involved. The spread in data during such measurements was found to be well within the accuracy limit.

4 Experimental Results and Discussion

Once the reproducibility and reliability of the experimental apparatus were demonstrated by using specimens of certified materials, the thermal conductivity of cobalt-based catalyst specimens was measured. The investigated specimens were described in Table 1. The theoretical density of a cobalt-based catalyst is normally in the range from $0.9091\,\mathrm{g\cdot cm^{-3}}$ to $0.9325\,\mathrm{g\cdot cm^{-3}}$. In the present study, a value of $0.9091\,\mathrm{g\cdot cm^{-3}}$ for the density of the fully dense material is used as a reference value to calculate the relative densities of the specimens. Porosity values are obtained by deducting the calculated values of the percentage theoretical density from 100.

For these investigations, we took four powder fractions: +360 mesh, $-360/+250$ mesh, $-250/+190$ mesh, and $-190/+80$ mesh. The specimens were pressed at different pressures. The thermal conductivity of the cobalt-based catalyst at various densities were determined as a function of temperature. The results are presented in Table 2 for a catalyst specimen made from $-250/+190$ mesh size particles with a density of $0.9091\,\mathrm{g\cdot cm^{-3}}$. The measurement results given in Table 2 (and the corresponding graphical presentation in Fig. 4) show that the thermal conductivity of cobalt-based catalyst specimens increases with temperature. In Table 2, R'' represents the total thermal resistance between the measurement points across the specimen. As can be seen in Table 2, the value of R'' had an opposite trend with increasing temperature. The total thermal resistance includes the thermal resistance of the specimen, the thermal resistance of the copper heat probe, and the thermal contact resistance at the interfaces between the specimen and the copper heat probes. Since the inner surfaces of the copper heat probes are smooth and they are in tight contact against the surfaces of the specimen, the thermal contact resistance is assumed to be negligible in this work. The thermal conductivity is then related to the temperature t_2.

Generally, the thermal conductivity of a solid has a linear relationship with temperature, thus,

$$\lambda = a + bt$$

The constants (a, b) were calculated by regression in terms of the experimental data of the catalyst specimen at different temperatures, namely, $a = 0.8652$, $b = 0.00108$, and $R = 0.99384$.

In order to observe the relations between a characteristic parameter and thermal conductivity, the measurement results are also presented in the form of plots of thermal conductivity against temperature, density, and porosity in Figs. 4, 5, and 6.

Table 2 Experimental results for the thermal conductivity of cobalt-based catalyst specimen ($\rho = 0.9091 \mathrm{g \cdot cm^{-3}}$)

t_1(°C)	t_2(°C)	t_3(°C)	t_4(°C)	$R''(\mathrm{km^2 \cdot W^{-1}})$	$\lambda(\mathrm{W \cdot m^{-1} \cdot ^\circ C^{-1}})$
194.8	176.9	73.5	71.3	37.645	1.06034
200.0	181.6	75.7	73.4	35.486	1.06447
207.5	188.4	78.8	76.2	35.467	1.06822
214.6	194.8	81.8	78.9	34.509	1.07469
219.8	199.4	83.2	80.1	34.068	1.07708
225.1	204.3	84.5	81.5	33.792	1.08525
231.4	209.5	86.2	83.1	33.690	1.08981
237.5	214.9	88.2	84.9	33.541	1.09484
243.1	219.8	89.6	86.3	32.448	1.09838
248.8	224.8	91.3	87.9	32.346	1.10463
254.2	229.6	93.5	89.6	32.228	1.11058
259.8	234.3	94.5	91.2	31.968	1.11995
265.7	239.5	96.8	92.9	31.848	1.12646
270.5	243.7	98.5	94.4	31.751	1.13088
275.6	248.1	99.8	95.5	31.635	1.13556

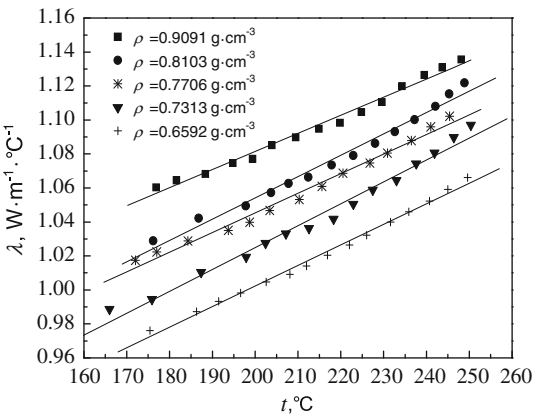

Fig. 4 Effect of temperature on thermal conductivity for cobalt-based catalyst specimens

Figure 4 indicates the temperature dependences of the thermal conductivity of specimens made from powders with fractions of $-250/+190$ mesh size by pressing. A regression fit was made to the experimental data. The effect of the density on the thermal conductivity is significant. The thermal conductivity increased when the densities of the specimens increased from $0.6592 \mathrm{\ g \cdot cm^{-3}}$ to $0.9091 \mathrm{\ g \cdot cm^{-3}}$.

Thermal conductivity values at different porosities for specimens made of three powder fractions are shown in Fig. 5. The mean temperature of the specimens is 200 °C. Since the relative error of the measurements is less than 5 %, the spread of the results for the different powder fractions lie within the uncertainty. As Fig. 5 indicates, the thermal conductivity is practically independent of the particle size of the powder.

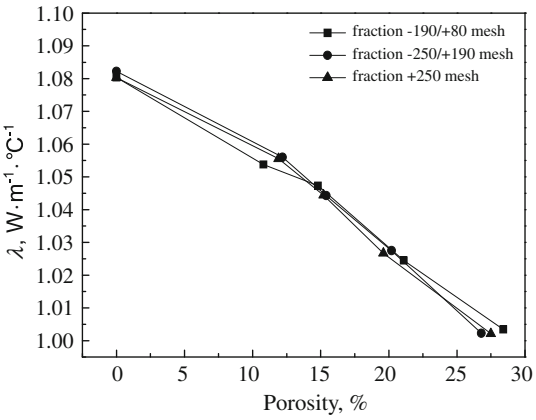

Fig. 5 Thermal conductivity versus porosity and powder size at 200 °C

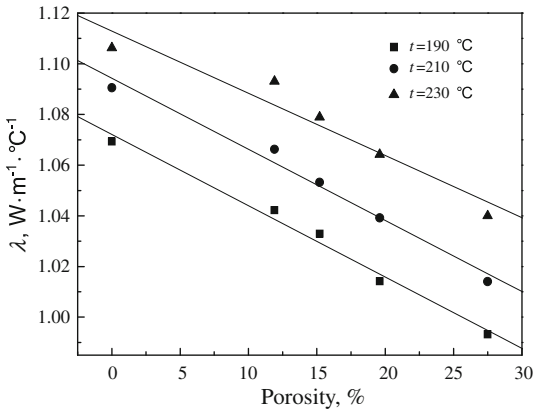

Fig. 6 Thermal conductivity versus porosity and temperature

We also demonstrated the influence of the porosity of specimens made of the same size powders on thermal conductivity. The relation of the thermal conductivity of the catalyst specimen as a function of the estimated porosity is shown graphically in Fig. 6 at temperatures of 190 °C, 210 °C, and 230 °C. The results of measurements were represented by approximately parallel straight lines. As can be seen from Fig. 6, a monotonic decrease in the thermal conductivity with increasing porosity was observed at three different temperatures. It is an opposite trend compared with the effect of density on the thermal conductivity. The increase in thermal conductivity with decreasing porosity was due to the greater compact heat transfer between the powder particles.

5 Effects of Measuring Factors

5.1 Specimen Thickness Effect

That the thermal conductivity of all the specimens examined differed only slightly confirmed that the specimen thickness had only a slight effect on the thermal conductivity. We also observed that if the specimen was too thick, side heat loss was increased;

Table 3 Thermal conductivities of different thickness specimens

Specimen number	Set temperature (°C)	Specimen temperature (°C)	Specimen thickness (mm)	Thermal conductivity ($W \cdot m^{-1} \cdot {}^{\circ}C^{-1}$)
7-1	330	188.5	3.547	1.02775
7-2	330	188.9	3.551	1.02953
7-3	330	188.7	3.498	1.03151
8-1	330	189.3	5.685	1.01448
8-2	330	189.1	5.712	1.02314
8-3	330	189.8	5.723	1.01996
9-1	330	191.3	8.153	1.02141
9-2	330	191.2	8.155	1.01698
9-3	330	191.2	8.176	1.01584

inversely, heat short-circuiting may be formed if too thin. So a certain requirement of thickness was needed.

As seen in Table 3, the thermal conductivity differences among specimens with thicknesses of 3 mm, 6 mm, and 8 mm were small. It was found that the relative difference was less than 2 %. Hence, specimens of 2 mm to 8 mm thickness may be considered as suitable specimens in the measurements.

5.2 Water Bath Temperature Effect

The effect of the water bath temperature on the thermal conductivity is shown in Table 4. From Table 4, it was observed experimentally that the thermal conductivity basically remained invariable at different water bath temperatures. The function of circulating cooling water was to remove heat for keeping the system temperature stable. Although the results showed that the water bath temperature had little effect on the results over a certain temperature range as long as the system could achieve a steady state, it does influence the time for reaching a thermal balance. This was confirmed by the observation that the time to reach steady state got longer with increasing water bath temperature.

Table 4 Effect of water bath temperature on thermal conductivity

Specimen number	Set temperature (°C)	Water bath temperature (°C)	Time to achieve steady state of system (min)	Thermal conductivity ($W \cdot m^{-1} \cdot {}^{\circ}C^{-1}$)
10	340	30	100–120	1.07569
		40	125–150	1.07708

5.3 Effect of Parallelism of Specimen

The effect of the parallelism of the specimen on the thermal conductivity is shown in Table 5. In order to observe the effect of nonparallelism on the thermal conductivity, contrast tests were carried out according to three different parallelisms of fabricated specimens. For these measurements, fresh specimens were fabricated from the same powder particles under the same compressing pressure in air. As seen from the test results and t-test analysis, the thermal conductivity decreased with an increase of the specimen surface slope. The thermal conductivity showed apparent differences when the slope exceeded 0.0333. This could be explained in that specimen nonparallelism leads to heat flow distortion and asymmetrical distribution of the surface temperature. Hence, the upper and lower surfaces of the specimen should be parallel and smooth to measure the thickness accurately and to reduce the errors.

5.4 Effect of Surface Roughness of Specimen

The effect of surface roughness of the specimen on thermal conductivity is clearly observed in Table 6. Surface rubdown and nonrubdown of specimen play an important role in the thermal conductivity measurement. The specimen surface was required to be smooth in order to eliminate the effect of an air layer on the experimental results. A steel-made ruler marginal examination method was used to measure the smoothness of the specimen. A qualified specimen was defined as no light passing the interface between the ruler and the specimen surface. A heat conduction medium should be besmeared during the measurement. As can be seen from the results in Table 6, the thermal conductivity of a nonrubdown specimen was less than that of a rubdown specimen. Here, it should be noted that the smoothness of specimens must be examined before the measurements.

Table 5 Thermal conductivity values of different parallelism specimens

Specimen number	Set temperature (°C)	Specimen temperature (°C)	Specimen slope	Thermal conductivity ($W \cdot m^{-1} \cdot {}^{\circ}C^{-1}$)
11-1	300	172	0	1.04867
11-2	300	173	0.0167	1.01525
11-3	300	172.6	0.0333	0.94193

Table 6 Thermal conductivity of different smoothness specimens

Specimen number	Smoothness	Thermal conductivity ($W \cdot m^{-1} \cdot {}^{\circ}C^{-1}$)
12-1	Rubdown	1.08423
12-2	Non-rubdown	0.96516

5.5 Moisture Content Effect

To check the effect of moisture content, an attempt was made to measure the thermal conductivity of specimens with 10 % to 50 % moisture content, which were fabricated from four powder fractions of the same mass and compressing pressure with increasing the temperature. The results tabulated in Table 7 showed that the thermal conductivity had a remarkable increase with increasing moisture content at the same set temperature. The main reason for this phenomenon is that a liquid bridge exists in the specimen, which makes the contact resistance decrease between the particle boundaries because the thermal conductivity of water is greater than that of air under normal pressure. In a macroscopic view, the thermal conductivity of a specimen increases.

In order to observe the effect of moisture content on the thermal conductivity at different temperatures, measurements were performed on the specimen with 10.25 % moisture content in air. For the measurement, a fresh specimen was fabricated from the same material. The results are shown in Fig. 7. The plot clearly demonstrates that for a specimen with 10.25 % moisture content, the effective thermal conductivity decreased with increasing temperature from 170 °C to 186 °C. Above 186 °C, the thermal conductivity increased with increasing temperature. This can be explained in that the moisture content in the probe adjacent region decreased because of evaporation and diffusion. However, the effect of the moisture content almost remained zero after the temperature reached a certain value. And then the thermal conductivity increased with

Table 7 Effects of moisture content on the thermal conductivity

Specimen number	Moisture content (%)	Set temperature (°C)	Thermal conductivity ($W \cdot m^{-1} \cdot {}^{\circ}C^{-1}$)
13-1	10.25	300	1.05321
13-2	20.63	300	1.08482
13-3	35.41	300	1.12354
14-4	49.25	300	1.16642

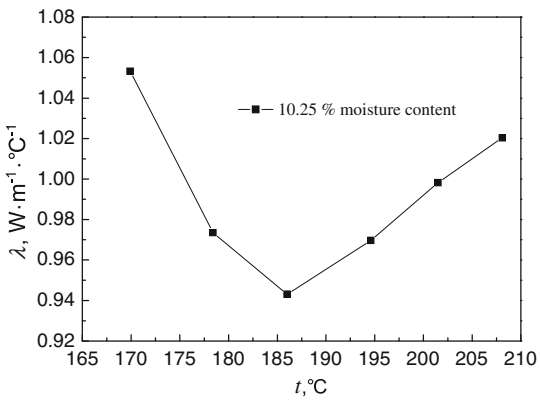

Fig. 7 Thermal conductivity of cobalt-based catalyst specimen with 10.25 % moisture content

increasing temperature. In summary, data have been determined showing the effect of moisture content on the thermal conductivity. Therefore, the specimens must be dried adequately to ensure reliability of the measured results.

6 Conclusions

An experimental apparatus and related procedures for the determination of the thermal conductivity of cobalt-based catalyst specimens, in the temperature range from 160 °C to 255 °C, are presented and discussed. The experimental apparatus used to determine the thermal conductivity provides data that show that the steady-state apparatus can yield measurements with an uncertainty of 5 %. The relative error, assessed in accordance with standards, for the thermal conductivity measurement on Teflon at 25 °C is 4.8 %. The steady-state apparatus is easy to operate and allows measurements to be made in a shorter time compared with other steady-state apparatuses. The measurement results demonstrated the reliability of the proposed technique.

On the basis of the measurements, the thermal conductivity of the specimens increases with increasing temperature and density. Meanwhile, the thermal conductivity is practically independent of the particle size of the powder. Data analysis reveals that the thermal conductivity of the specimens decreases with increasing porosity. In addition, the effects of some other factors on the thermal conductivity were studied and discussed. The results showed that parallelism, roughness and moisture content all had a significant influence on the reliability of the thermal conductivity measurements, whereas the specimen thickness and water bath temperature had only a slight influence on the thermal conductivity. Therefore, before measurements we need to consider these influence factors, which have been confirmed by testing to result in significant errors.

Acknowledgment The authors gratefully acknowledge the financial support from the research program of SINOPEC, China (No.107035).

References

1. R.A. Sehr, Chem. Eng. Sci. **2**, 145 (1958)
2. J.B. Butt, AIChE J. **11**, 106 (1965)
3. C.S. Sharma, P. Harriott, R. Hughes, Chem. Eng. J. **10**, 73 (1975)
4. R.A. Mischke, J.M. Smith, Ind. Eng. Chem. Fundam. **1**, 288 (1962)
5. S. Masamune, J.M. Smith, Ind. Eng. Chem. Fundam. **2**, 136 (1963)
6. G. Groppi, G. Airoldi, C. Cristiani, E. Tronconi, Catal. Today **60**, 57 (2000)
7. G.S. Yu, J.G. Yu, Z.H. Yu, Chem. Eng. **28**, 22 (2000)
8. R. Barea, M.I. Osendi, J.M.F. Ferreira, P. Miranzo, Acta Mater. **53**, 3313 (2005)
9. K.Y. Sastry, L. Froyen, J. Vleugels, E.H. Bentefour, C. Glorieux, Int. J. Thermophys. **25**, 1611 (2004)
10. N. Atabaki, B.R. Baliga, Heat Mass Transfer **44**, 85 (2007)
11. C.G.S. Pillai, A.M. George, Int. J. Thermophys. **12**, 563 (1991)
12. G.A. Longo, Int. J. Thermophys. **29**, 664 (2008)
13. U. Hammerschmidt, Int. J. Thermophys. **23**, 1551 (2002)
14. Q.F. Mang, R.S. Fang, L.C. Ling, S. Guo, *Practical Property Manual of Thermophysics* (China Press of Agriculture and Machinery, Beijing, China, 1986), pp. 380–400